Available online at www.sciencedirect.com
SCIENCE DIRECT
Journal of Controlled Release 111 (2006) 47 – 55
journal of controlled release
www.elsevier.com/locate/jconrel

Intestinal uptake and biodistribution of novel polymeric micelles after oral administration

Frédéric Mathot [a], L. van Beijsterveldt [b], V. Préat [a,*], M. Brewster [b], A. Ariën [b]

[a] Université Catholique de Louvain, Department of Pharmaceutical Technology, Avenue E. Mounier 73 UCL 73.20, 1200 Brussels, Belgium
[b] Johnson and Johnson, Pharmaceutical Research and Development, Division of Janssen Pharmaceutica, 2340 Beerse, Belgium

Received 5 August 2005; accepted 21 November 2005

Abstract

To determine the fate of polymeric micelles after oral administration, we investigated the possible transport of polymeric micelles across Caco-2 monolayers and their biodistribution in rats after per os administration of [^{14}C]-labelled mmePEG$_{750}$P(CL-co-TMC) micelles containing risperidone (BCS Class II drug). mmePEG$_{750}$P(CL-co-TMC) was able to cross Caco-2 monolayer via a saturable transport mechanism. The oral bioavailability of the polymer was 40%. Polymeric micelles based on mmePEG$_{750}$P(CL-co-TMC) showed very low clearance by the reticuloendothelial system (RES) and a renal excretion. A sustained release of risperidone was observed.
© 2005 Elsevier B.V. All rights reserved.

Keywords: Self-assembling polymeric micelles; Caco-2; Risperidone; Oral delivery; Biodistribution; mmePEG$_{750}$P(CL-co-TMC)

1. Introduction

The advent of high-throughput screening has affected contemporary drug pipeline based in large part on the nature of the assay which includes the evaluation of DMSO solution of drug candidates in immobilized receptor matrices. As a result, new drug leads tend to be more lipophilic. On top of this, the hit to lead process reduces still further aqueous solubility meaning that the formulator is often faced with significant challenges with regard to generating appropriately orally bioavailable dosage forms. As defined by the Noyes–Whitney equation, dissolution rate varies as a function of particle size, wettability and saturation solubility meaning that for compounds whose oral bioavailability is solubility or dissolution rate limited (i.e., BCS Class II compounds), any factor that improves solubility will improve bioavailability. Different strategies can be used to augment the water solubility of drug candidates in this regard including the use of chemical modification and physical form manipulation such as (1) the use of different salts and polymorphs as well as prodrugs, (2) the conversion of the material into amorphous dispersion or solid solutions, and (3) micronization or nanonization. A second widely used technique is through modification of the solubilization medium by using co-solvents, complexing agents (i.e., cyclodextrins) or surfactants [1].

In an aqueous medium, above a given concentration termed the critical micellar concentration (CMC), surfactants self-assemble into a colloidal dispersion of molecular aggregates called micelles (<50–100 nm) [2], and have been shown to solubilize hydrophobic drugs inside the core formed by the lipophilic part of the surfactant. The hydrophilic moieties form the shell or corona of this nanocarrier [2–6]. In addition to the increase in drug solubility, micelles can protect the incorporated drugs by insulating them from the aqueous environment.

Besides classic surfactants, micelles can also be formed from amphiphilic polymers. These polymers often provide better kinetic and thermodynamic stability than conventional surfactants [2–6]. However, they exhibit a number of disadvantages including a complex manufacturing process which requires organic solvents followed by a dialysis step or an evaporation process depending on polymer polarity [3–6]. These limitations were addressed by the introduction of self-assembling polymeric micelles such as mmePEG$_{750}$P(CL-co-TMC) [monomethyletherpoly(oxyethylene glycol$_{750}$)-poly(caprolactone-co-trimethylene carbonate)]. This amphiphilic copolymer aggregates spontaneously into 20 nm micelles upon contact with

* Corresponding author. Tel.: +32 2 764 73 20; fax: +32 2 764 73 98.
E-mail address: preat@farg.ucl.ac.be (V. Préat).

0168-3659/$ - see front matter © 2005 Elsevier B.V. All rights reserved.
doi:10.1016/j.jconrel.2005.11.012

water [7] and is intended for oral delivery of poorly soluble drugs.

The aims of the present work were to determine whether or not a polymeric excipient forming spontaneously micelles, mmePEG$_{750}$P(CL-co-TMC), crosses the intestinal barrier as well as to study the fate of this excipient after oral and parenteral administration. Hence, [^{14}C]-radiolabelled ε-caprolactone was introduced during the polymer synthesis into the mmePEG$_{750}$P(CL-co-TMC) block copolymer structure. Caco-2 cells, a well recognized in vitro model for estimation of intestinal drug permeability [8], were exploited to elucidate the kinetics of cell penetration of mmePEG$_{750}$P(CL-co-TMC). Rats were used as an in vivo model in order to evaluate the pharmacokinetic parameters of both the polymer and the drug entrapped in the polymeric micelles (Fig. 1). Risperidone served as a BCS Class II model drug to assess the potential beneficial solubilizing aspects for the polymeric micelles [9,10].

2. Materials and methods

2.1. Synthesis and characterization of polymers

The mmePEG$_{750}$P(CL-co-TMC) (50/50 molar ratio) polymers were synthesized by J and J-Center for Biomaterials and Advanced Technologies (CBAT, Somerville, NJ, USA). Monomethyl ether polyethylene glycol with a chain length of 750 g/mol (mmePEG$_{750}$) was purchased from Fluka (Milwaukee, WI, USA). ε-Caprolactone (CL) was purchased from Union Carbide (Danbury, CT, USA), and trimethylene carbonate (TMC) from Boehringer Ingelheim (Petersburg, VA, USA). Stannous octoate and toluene were obtained from Aldrich (Milwaukee, WI, USA). [^{14}C]-labelled mmePEG$_{750}$P(CL-co-TMC) (50/50 molar ratio) polymers were synthesized by Perkin Elmer employing ε-[caprolactone-2,6-^{14}C].

The synthesis of mmePEG$_{750}$P(CL-co-TMC) diblock copolymer was performed by ring opening polymerization as described earlier by Ould-Ouali et al. [7,11,12]. The same procedure was applied for the [^{14}C]-labelled mmePEG$_{750}$P(CL-co-TMC) synthesis except ε-[caprolactone-2,6-^{14}C] was used instead of unlabelled ε-caprolactone (on a mole basis).

The polymer composition and residual monomer content were analysed by proton NMR. Gel permeation chromatography was used to determine the molecular weight and the polydispersity of the polymers.

The radiochemical purity of [^{14}C]-mmePEG$_{750}$P(CL-co-TMC) was checked. This analysis was carried out using a Modular Gilson HPLC system equipped with a Type 305 pump, a slave pump (type 306), a manometric module (model 805) and a dynamic mixer (model 811). Compounds were separated on a Styragel® column HR 4E 7.8 × 300 mm using a THF mobile phase, a flow rate of 1.00 ml/min and a sample volume of 4 μl. These conditions gave a retention time of 8.00 min. The Berthold radioactivity detector lb 506 C-1 was adjusted to a flow rate of 5.0 ml/min (4 ml scintillation fluid + 1 ml eluent from column) using a Z-500 flow cell. The energy channels of the radioactivity detector were LL25 and UL999. The sample was prepared by dissolving 60 mg of [^{14}C]-mmePEG$_{750}$P(CL-co-TMC) in 1 ml THF.

2.2. Physicochemical characterization of micelles

The self-assembling properties of the copolymers were assessed by adding water, gradually, under gentle stirring at 37 °C [7].

The particle size and ζ potential of the micelles were determined, respectively, by photon correlation spectroscopy (PCS) and laser Doppler velocimetry combined with phase analysis light scattering (PALS) using a Zetasizer® Nano ZS (Malvern Instruments, UK). The measurements were performed in citrate–citric acid buffer pH 6.0 (300 mOsm/kg).

The critical micellar concentration (CMC) of the polymer was determined based on the emission spectrum of pyrene [7].

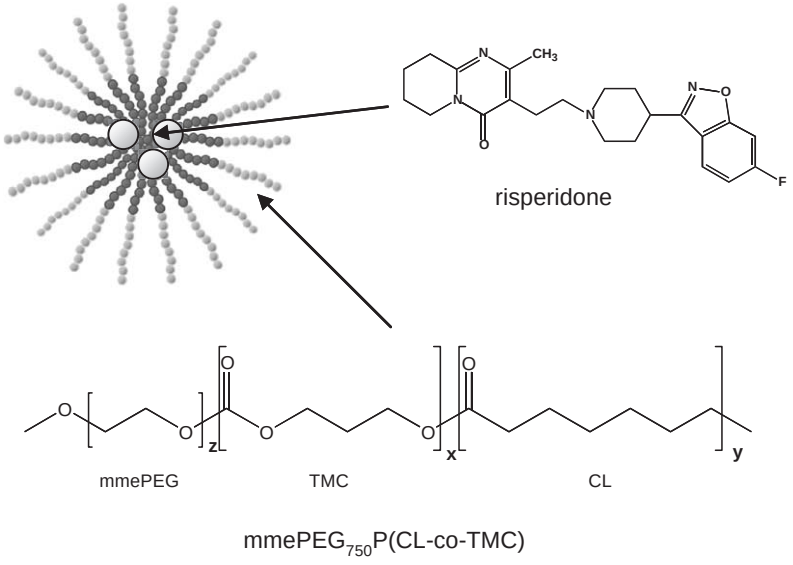

Fig. 1. Representation of the structure of risperidone, mmePEG$_{750}$P(CL-co-TMC) and polymeric micelles.

2.3. Permeation kinetics of mmePEG$_{750}$P(CL-co-TMC) in the in vitro model

2.3.1. In vitro formulation

For the in vitro experiments, solutions of 0.05%, 0.005% and 0.001% polymer were prepared by mixing an appropriate amount of [^{14}C]-labelled mmePEG$_{750}$P(CL-co-TMC) with citrate–citric acid buffer pH 6.0 (300 mOsm/kg) for 1 h. Micellar solutions of 0.5%, 3% and 10% were prepared by mixing unlabelled polymer with radiolabelled polymer solution. Moreover, risperidone at 0.3 mg/ml (Janssen Pharmaceutica, Beerse, Belgium) was solubilized in the 10% polymer solution in order to have the same formulation used for oral administration to rats in the in vivo study.

2.3.2. Cell culture

Caco-2 cells were obtained from the American Type Culture Collection (ATCC), and were used between passage 62 and 71. The cultures were mycoplasma-free (mycoplasma detection kit; Roche Gmbh, Mannheim, Germany). The cells were routinely maintained in plastic culture flasks of 162 cm^2 (Corning Incorporated, NY, USA) with 0.2 μm vent cap. The cells were subcultivated before reaching confluence. Caco-2 cells were harvested with 0.25% trypsin and 0.2% EDTA (5–15 min) at 37 °C and seeded in new flasks. The culture medium, Dulbecco's Modified Eagle Medium (DMEM), was supplemented with 1% non-essential amino acids (NEAA), 2 mM L-glutamine, 100 U/ml penicillin/streptomycin and 10% fetal bovine serum (FBS). All supplements and cell culture media were purchased from InVitrogen (Merelbeke, Belgium).

2.3.3. TEER measurement

Measurement of trans-epithelial electrical resistance (TEER) was used to determine the integrity of cell monolayers. The TEER monolayer was measured at 37 °C using an Evom resistance voltohm meter (World Precision Instruments, Berlin, Germany). Only cell monolayers having TEER values above 400 Ω cm^2 were used in these experiments.

2.3.4. Transport experiments

Caco-2 monolayers were grown in the Transwell polycarbonate inserts (12 mm insert diameter, 0.4 μm pore size) (Corning Costar, Cambridge, U.K.) for a period of 21 days, at a seeding density of 1.5×10^5 cells/cm^2. The culture medium was exchanged every two days for 21 days. For transport experiments, the cell monolayers were washed with Hanks' balanced salt solution (HBSS) supplemented with FBS 1% (v/v) (0.5 ml in the apical compartment and 1.5 ml in the basolateral side) twice within 30 min at 37 °C. For the apical to basolateral transport, the buffer was removed from the cells and replaced with 500 μl of the test compound (mmePEG$_{750}$P(CL-co-TMC) solutions) on the apical side. The monolayers were incubated for 120 min at 37 °C. At 0 and 120 min, the electrical resistance was measured. The amount of polymer crossing the monolayer was assayed by removing 1.5 ml of buffer from the basolateral compartments after 30, 60, 90 and 120 min. Each sample was placed in 12 ml of Aqualuma (Lumac, Groningen, The Netherlands) which served as the scintillation medium.

The amount of risperidone crossing the Caco-2 monolayer was determined by HPLC-UV as described earlier [13]. The transport experiments were performed at least in triplicate.

2.3.5. Measure of [^{14}C]-mmePEG$_{750}$P(CL-co-TMC) transport

The amounts of polymer crossing the monolayers were determined by liquid scintillation counting using a Wallac 1410 Liquid Scintillation Counter (Pharmacia) with automatic external standardization. A standard curve was generated for both high and low concentrations of mmePEG$_{750}$P(CL-co-TMC) (from 0.1% to 10.0%; $R^2 \sim 1$ and from 0.001% to 0.1%; $R^2 = 0.9998$, respectively).

The transport rate (dQ/dt) was calculated by plotting the amount of polymer penetrating the basolateral side versus time (30, 60, 90 and 120 min) and then determining the slope of this relationship. The apparent permeability coefficient (P_{app}, cm sec^{-1}) was calculated from the following equation:

$$P_{app} = \frac{dQ/dt}{C_0 \cdot A}$$

where dQ/dt is the permeability (mg/sec), C_0 is the initial polymer concentration on the apical side of cell monolayers (mg/ml), and A is the surface area of the membrane filter in cm^2 [13,14].

2.4. Pharmacokinetics and biodistribution of mmePEG$_{750}$P(CL-co-TMC) and risperidone after intravenous and oral administration

2.4.1. In vivo formulations

The intravenous formulation contained 1.5 mg/ml risperidone and 10% mmePEG$_{750}$P(CL-co-TMC) at a concentration of 21.70 μCi/ml and was prepared by mixing 823 mg of unlabelled polymer with 15 mg of risperidone in 9 ml of Ultrapure water for 24 h at room temperature. This solution was then added to 192.1 mg of [^{14}C]-polymer and allowed to mix for another 3 h at room temperature. The formulation for oral administration contained 0.3 mg/ml risperidone and 10% mmePEG$_{750}$P(CL-co-TMC) at a concentration of 4.20 μCi/ml and was prepared by mixing 4.823 g of unlabelled polymer with 15 mg of risperidone in 45 ml of Ultrapure water for 24 h at room temperature. This solution was then added to 185.9 mg [^{14}C]-polymer and allowed to mix for another 3 h at room temperature.

Total radioactivity of the formulations was determined by liquid scintillation spectrometry using a Packard microprocessor controlled multi-user liquid scintillation system (Packard model Tri-Carb® 2100 TR or 1900 TR/CA) with automatic external standardization. The concentration of risperidone in the formulations was confirmed by HPLC with UV-detection according to the protocol described by Ould-Ouali et al. [13].

2.4.2. In vivo experiments

Twenty-one male Sprague–Dawley rats were obtained from Charles River (Sulzfeld, Germany) and were maintained in a facility using procedures in accordance with appropriate

Belgian legislation. Immediately prior to dosing, the animals intended for oral administration had a recorded mass of 265 ± 3 g (n = 9) and the animals for intravenous administration, 267 ± 12 g (n = 12). After an acclimatization period of four days, the animals were dosed orally by gavage at a level of 1 ml of the drug formulation per 100 g body weight or intravenously via the tail vein at a dose of 0.2 ml per 100 g body weight. Both formulations contained 10% mmePEG$_{750}$P(CL-co-TMC) and 0.3 (oral) or 1.5 mg/ml (intravenous) risperidone corresponding to a dose of 1.0 (oral) or 0.2 g/kg (intravenous) mmePEG$_{750}$P(CL-co-TMC) and 3 mg/kg risperidone. Rats were kept in stainless steel metabolism cages with tap water and food provided ad libitum. Urines were collected.

Blood samples (in a 2 ml EDTA Vacutainer Tubes (Becton Dickinson, Temse, Belgium)) were taken for plasma separation via retro-orbital venous plexus puncture from the rats at 7 min (intravenous only), 20 min, 1, 3, 8, 24, and 72 h after dosing. Blood was centrifuged for 10 min at room temperature at approximately 1900 × g. Plasma was separated and stored at −20 °C until analysis. Following the last blood collection, animals were sacrificed and liver, kidneys and spleen were removed. Tissues were weighed and placed in labelled, tarred Petri dish and stored at −20 °C until analysis.

2.4.3. Radioactivity determination in tissues and urines

Radioactivity associated with labelled mmePEG$_{750}$P(CL-co-TMC) was measured using a liquid scintillation spectrometer, Packard 2100 TR or Packard 1900 TR/CA with Ultima Gold® (Packard) serving as the scintillation medium. After thawing, liver, kidney and spleen were homogenised in demineralized water (1/4, w/v or +5 ml if tissue weight <1 g), using a Polytron® Kinematica homogeniser. Duplicate aliquots of 0.2 ml of the tissue homogenates were diluted to 1.0 ml total volume with demineralized water and counted for total radioactivity after addition of 10 ml of Ultima Gold®. Duplicate aliquots of 0.2 ml of plasma were counted for total radioactivity after dilution to 1.0 ml total volume with demineralized water and the addition of 10 ml of Ultima Gold®. Levels of total radioactivity were calculated as micrograms or nanograms of mmePEG$_{750}$P(CL-co-TMC) per milliliter plasma or per gram of wet tissue, as well as percent of the administered dose.

Urines were collected after 8, 24 and 48 h upon oral and intravenous administrations. At each time interval, the volume of urine for each rat was measured. Aliquots of 250 μl were placed in 12 ml of Aqualuma™ and analysed by liquid scintillation.

2.4.4. Pharmacokinetics of risperidone and 9-hydroxyrisperidone

All plasma samples were analyzed for unchanged risperidone and its 9-hydroxy metabolite by means of a validated LC-MS/MS-method [13,15]. Solid phase extraction was performed prior to LC-MS/MS in order to isolate drugs from the plasma. In brief, 2 ml of 0.1 M phosphate buffer pH 6.0 was added to plasma samples (0.1 ml), followed by the addition of an internal standard and 100 μl of methanol. Samples were eluted on a Bond Elut Certify column (10 cm^3, SPE Varian, Sint-Katelijne Waver, Belgium) which were prepared using 1 ml of 0.1 M phosphate buffer. After application, the columns were washed with water, methanol, and 1 M acetic acid prior to elution of the active molecules with 3 ml methanol–NH_4OH (25%; 98/2 v/v). After evaporation of the samples to dryness, the residues were reconstituted in 300 μl 0.01 M ammonium formate pH 4.0/Acetonitrile (50/50 v/v). Twenty microliter aliquots of the supernatant were injected onto a reversed-phase LC-column (Hypersil BDS C18 3 μm, 100 × 4.6 mm; Alltech, Lokeren, Belgium) after vortexing.

LC-MS/MS analysis was carried out on an API-3000 MS/MS (Applied Biosystems, Belgium) spectrometer, coupled to an HPLC-system (Agilent Technologies, Diegem, Belgium). The MS/MS operated in the positive ion mode using a TurboIonSpray™-interface (electrospray ionization) and was optimized for the quantification of risperidone and 9-hydroxyrisperidone. The linear dynamic range of the calibration curves ranged from 0.5 to 1250 ng/ml for the two compounds. The inter- and intrabatch accuracy was between 85% and 115% of the nominal value over the entire range. The precision was within 15% over the entire range [13,15] with a lower limit of quantification limit (LLOQ) of 0.5 ng/ml for both analytes.

Plasma concentrations were subjected to a non-compartmental pharmacokinetic analysis (NCA) using validated WinNonlin software (WinNonlin Release 4.0.1a Enterprise, Pharsight Corporation, Mountain View, California, U.S.A.). Reported pharmacokinetic parameters were estimated in this NCA. AUC values were calculated using the linear trapezoidal rule from 0 to t (last blood or tissue sampling time) with extrapolation to infinite time. AUC_{0-t}-values of radioactivity in tissues were compared with those in plasma by calculation of the ratios. The bioavailability (Fabs) after oral administration of mmePEG$_{750}$P(CL-co-TMC) micelles versus after intravenous administration was calculated for unchanged risperidone and the active moieties (=risperidone+9-hydroxyrisperidone).

2.5. Statistical analysis

For all experiments, data are presented as the mean ± SD. Statistical analyses for in vitro experiments were done using JMP software (SAS Institute Inc., version 4.0.2). Significance was tested using Wilcoxon/Kruskal–Wallis test (ChiSquare). Values of $p < 0.05$ were considered statistically significant. A t-test was applied for the trans-epithelial electrical resistance (TEER) differences. Values of $p < 0.05$ were considered statistically significant. Concerning the in vivo experiments, pharmacokinetic analysis was performed on mean data points, or on median values if not all corresponding levels of the same group, time points and tissue (n = 3) are higher than the limit of quantification. Tests for significant differences between the groups were done using Wilcoxon/Kruskal–Wallis test (ChiSquare) with JMP software (SAS Institute Inc., version 4.0.2). Values of $p < 0.05$ were considered statistically significant.

3. Results

3.1. Characterization of polymers and formulations

The diblock copolymers were synthesized by ring polymerization of CL and TMC initiated with monomethoxy end-capped PEG in presence of tin octoate as catalyst. The chemical composition as determined by proton NMR was in good agreement with the ratio of the monomers charged. Indeed, the CL/TMC molar ratio for mmePEG$_{750}$P(CL-co-TMC) was 49/49 mol/mol. The residual monomer content was less than 1 mol%. The weight-averaged molecular weight (Mw) of mmePEG$_{750}$P(CL-co-TMC) and [^{14}C]-mmePEG$_{750}$P(CL-co-TMC) were 5320±505 Da (PD=1.9±0.1; n=4) and 5188 Da (PD=1.6), respectively. The [^{14}C]-mmePEG$_{750}$P(CL-co-TMC) polymer had a radiochemical purity of ≥97%.

mmePEG$_{750}$P(CL-co-TMC) block copolymers formed spontaneously micelles [7,13]. Their size and ζ potential were found to be 24.15 nm (PDI: 0.052) and −2.7 mV (width: 13.2), respectively. The size measured in the apical medium was not influenced by the concentration of the polymer. The CMC of mmePEG$_{750}$P(CL-co-TMC) was 12.0±1.5 μg/ml. The measured concentrations of risperidone and polymer in the formulations tested were within 2% and 3% of the calculated concentrations, respectively.

3.2. Permeation of mmePEG$_{750}$P(CL-co-TMC) in an in vitro model

To assess whether polymeric micelles are able to cross a model for the intestinal barrier, Caco-2 cells were incubated with various concentrations of [^{14}C]-radiolabelled mmePEG$_{750}$P(CL-co-TMC) (0.001–10%) at the apical side.

The amount of polymer crossing the Caco-2 monolayers as function of time showed linear passage kinetics for all concentrations studied, as illustrated in Fig. 2. The higher the polymer concentration applied at the apical side, the greater the basolateral recovery. However, permeation was not proportional to the apical concentration. For polymer concentrations at the CMC (0.001%), the apparent permeability coefficient (P_{app}) was around 2.3×10^{-5} cm s^{-1}. The P_{app} decreased dramatically to reach a value between 2.5×10^{-6} and 0.58×10^{-6} cm s^{-1} for polymer concentrations well above the CMC of the copolymer (between 0.5% and 10%) as illustrated in Fig. 3. This phenomenon was also illustrated by the percentage of mmePEG$_{750}$P(CL-co-TMC) having crossed the monolayer. Approximately 37% of the radiolabelled polymer in the 0.001% solution was recovered at the basolateral site after 2 h while only about 1% was recovered for the 10% polymer solution. Concerning the risperidone entrapped in the 10% polymer formulation, its P_{app} was around 22 times higher than the polymer P_{app} at 10% ($1.29\times10^{-5}\pm6.1\times10^{-7}$ cm s^{-1}).

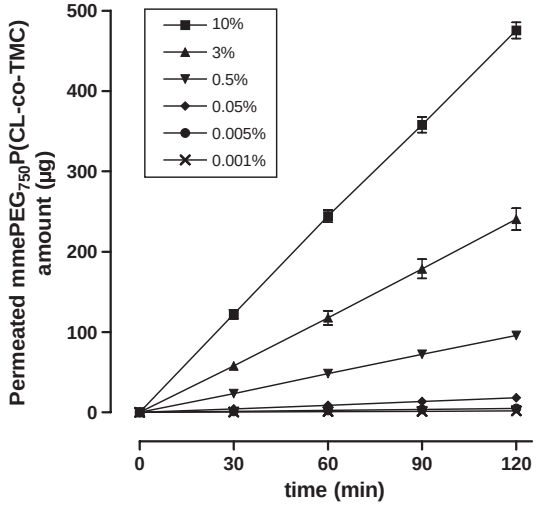

Fig. 2. Permeation of mmePEG$_{750}$P(CL-co-TMC) through Caco-2 monolayer. Curves represent cumulated amount of polymer found in the basolateral side after application of polymer solutions at the apical side as function of time (mean±SD, n=3).

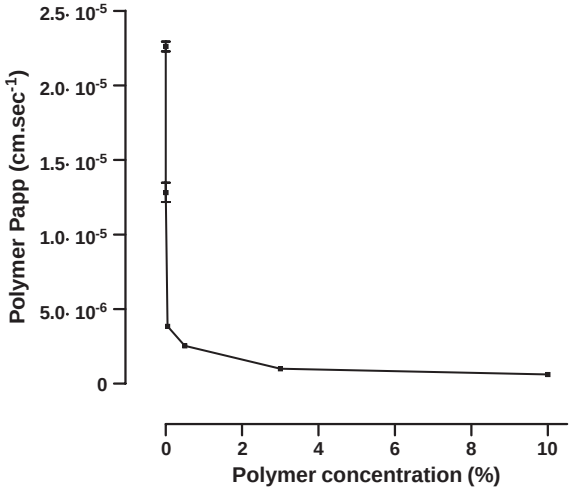

Fig. 3. Apparent permeability coefficient (P_{app}) of mmePEG$_{750}$P(CL-co-TMC) through Caco-2 monolayer from apical to basolateral side as function of polymer concentration (mean±SD, n=3).

The monolayer integrity was evaluated by measuring the trans-epithelial electrical resistance (TEER) before and after the kinetic study. No significant differences in TEER were observed for the 15 wells during the course of the experiment even at a 10% polymer concentration (t-test; $p>0.05$).

3.3. In vivo absorption and biodistribution of mmePEG$_{750}$P(CL-co-TMC) micelles and risperidone

Once evidence of mmePEG$_{750}$P(CL-co-TMC) passage across an in vitro model of the intestine was obtained, an in vivo study in rats was performed to evaluate the absorption and biodistribution of both polymeric micelles and risperidone entrapped within these micelles after a single intravenous or oral administration. The highest polymer concentration applied on Caco-2 cells (10% w/v) was used.

3.3.1. mmePEG$_{750}$P(CL-co-TMC) pharmacokinetics, biodistribution and elimination

Plasma levels after intravenous administration of the [^{14}C]-mmePEG$_{750}$P(CL-co-TMC) formulation at a dose of 0.2 g/kg

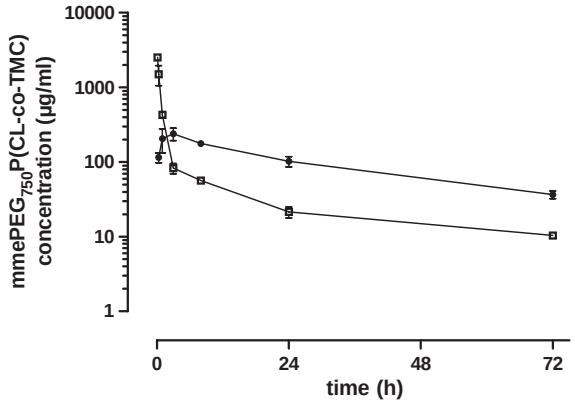

Fig. 4. Plasma profiles of total mmePEG$_{750}$P(CL-co-TMC)-related radioactivity after a single oral (●) and intravenous administration (□) of 3 mg/kg risperidone solubilized in 10% [^{14}C]-mmePEG$_{750}$P(CL-co-TMC) solution (1.0 and 0.2 g/kg for oral and intravenous formulation, respectively) in male Sprague–Dawley rat (mean±SD, n=3).

polymer were 2513±127 µg/ml of the total radioactivity at the first investigated time point, i.e., 7 min, after administration (Fig. 4). The total radioactivity concentration declined rapidly to 82.8±12.9 µg/ml at 3 h after administration and more gradually thereafter. At 72 h, the plasma levels of the mmePEG$_{750}$P(CL-co-TMC)-related radioactivity were 10.4±0.7 µg/ml.

After oral administration of the 1 mg/kg of [^{14}C]-mmePEG$_{750}$P(CL-co-TMC) formulation, plasma levels of total radioactivity increased to a peak value of 238±45 µg/ml at 3 h after administration. Thereafter mmePEG$_{750}$P(CL-co-TMC)-related radioactivity declined gradually. The dose normalized AUC_{0-72h}-ratio for the total radioactivity was estimated at 0.40 (Table 1).

Maximum tissue concentrations of mmePEG$_{750}$P(CL-co-TMC)-related radioactivity were observed at the first investigated time point after administration (i.e., 3 h after intravenous and 8 h after oral) and thereafter showed a gradual decline. Tissue to plasma ratios were 2.8 and 4.7 for liver, 2.9 and 3.4 for kidney and 1.3 and 2.0 for spleen, after oral and intravenous administration, respectively. At peak concentrations, liver levels represented 7.3% of the total administered dose after intravenous and 2.2% of the total administered dose after oral

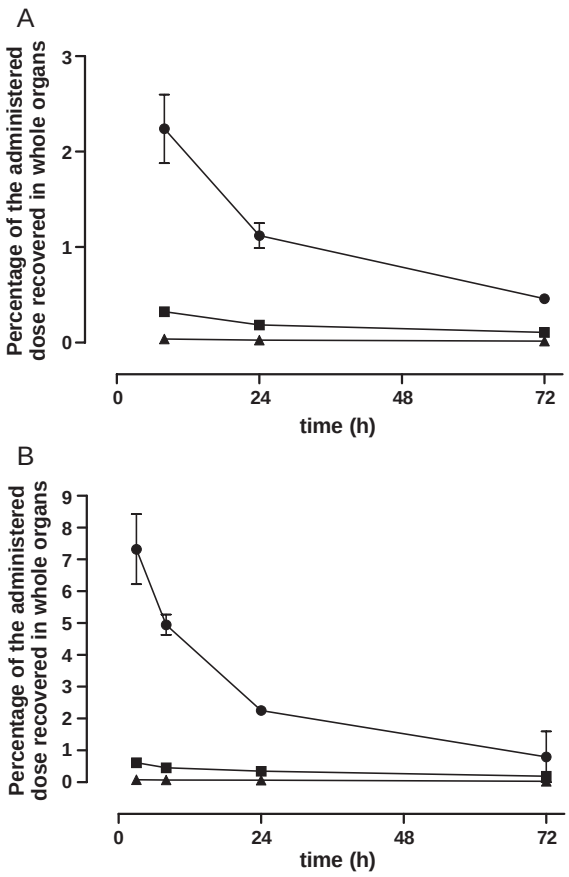

Fig. 5. (A) and (B) Mean tissue levels of total mmePEG$_{750}$P(CL-co-TMC)-related radioactivity as a percentage of total dose after oral (A) or single intravenous (B) administration of 3 mg/kg risperidone in a 10% mmePEG$_{750}$P(CL-co-TMC) solution (1.0 g/kg and 0.2 g/kg for oral and intravenous formulation, respectively) in male Sprague–Dawley rat. Liver (●), kidney (■) and spleen (▲) (mean±SD, n=3).

administration, as shown in Fig. 5A and B. At 72 h, these values decreased to 0.80% and 0.46%, respectively.

Urinary excretion of mmePEG$_{750}$P(CL-co-TMC)-related radioactivity after intravenous injection was 82.6%±10.2% of the administered dose within 8 h and reached 85.7%±13.9% after 24 h as shown in Fig. 6. After the oral delivery, 21.8%±7.5% of the administered dose was excreted in the urine after 8 h and raised to 38.6%±10.4% after 24 h.

Table 1
Pharmacokinetic parameters of total radioactivity after single intravenous and oral administration of 3 mg/kg risperidone in a 10% solution of [^{14}C]-mmePEG$_{750}$P(CL-co-TMC) micelles (1.0 and 0.2 g/kg for oral and intravenous formulation, respectively) in male Sprague–Dawley rat (mean±SD, n=3)

Tissue	Oral administration				Intravenous administration			
	Plasma	Liver	Kidney	Spleen	Plasma	Liver	Kidney	Spleen
T_{max} (h)	3	8[a]	8[a]	8[a]	–	3[a]	3[a]	3[a]
$t_{1/2\ 8-72\ h}$ (h)	29	–	–	–	28	–	–	–
C_{max} (µg-eq/ml or g)	238±45	591±98	423±15	148±6	3319[b]	362±46	170±13	70.8±10.5
$AUC_{0-72\ h}$ (µg-eq h/ml or g)	6840	–	–	–	3412	–	–	–
Dose norm. $AUC_{0-72\ h}$-ratio	0.40	–	–	–	–	–	–	–
$AUC_{t_{1-72\ h}}$ (µg-eq h/ml or g)[c]	5240	14,750	14,929	6979	1656	7723	5669	3334
$AUC_{t_{1-72\ h}}$ tissue/plasma ratio	(1.00)	2.81	2.85	1.33	(1.00)	4.66	3.42	2.01

[a] First sampling time point.
[b] Extrapolated concentration at time t=0 (C_0).
[c] t_1 is 8 h after oral and 3 h after intravenous administration.

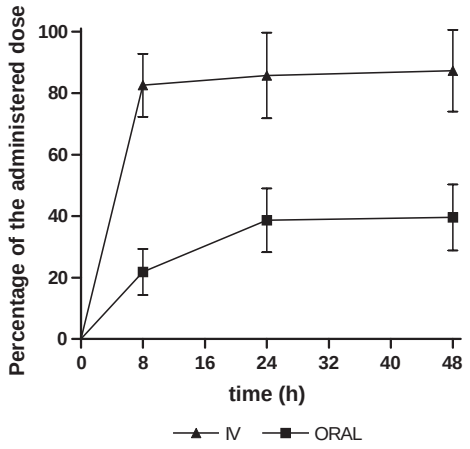

Fig. 6. Urinary excretion of total mmePEG$_{750}$P(CL-co-TMC)-related radioactivity as a percentage of total dose after oral (■) or single intravenous (▲) administration of 3 mg/kg risperidone in a 10% solution of mmePEG$_{750}$P(CL-co-TMC) in male Sprague–Dawley rat (mean±SD, n=6).

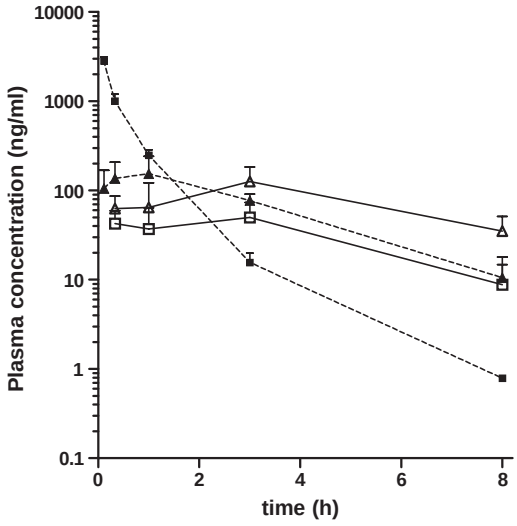

Fig. 7. Plasma profile of unchanged risperidone (□) and metabolically formed 9-hydroxyrisperidone (△) after single oral (empty symbol) and intravenous administration (full symbol) of 3 mg/kg risperidone in a 10% solution of mmePEG$_{750}$P(CL-co-TMC) in male Sprague–Dawley rat (mean±SD, n=3).

3.3.2. Risperidone and 9-hydroxyrisperidone pharmacokinetics

After intravenous administration of the polymer-risperidone formulation, rats were clearly sedated suggesting that risperidone was readily available from the micelles. One of the intravenously dosed animals died at about 1 h after injection. High initial plasma concentrations were observed for unchanged risperidone after intravenous administration and declined in a biphasic manner with a terminal $t_{1/2}$ of 1.2 h (Table 2). The total plasma clearance was estimated at 2.2 l/h/kg and the volume of distribution (Vd_{ss}) was 3.6 l/kg. Levels of the major (active) metabolite, 9-hydroxyrisperidone, increased to a peak value of 154±88 ng/ml at 1 h after administration and declined thereafter (Fig. 7). This diminution was slightly more gradual than that of risperidone itself, with a $t_{1/2}$ of 1.7 h. After 3 h, plasma levels of the 9-hydroxy metabolite were higher than those of risperidone itself; having said this the metabolite to unchanged risperidone AUC ratio was significantly less than 1 (0.39).

After oral administration, maximum plasma concentrations of both risperidone and its 9-hydroxy metabolite were observed at 3 h, and amounted to 50.0±23.6 ng/ml for risperidone and 126±57 ng/ml for the metabolite. Thereafter, plasma levels of both compounds gradually declined with $t_{1/2}$ of 2.0 and 2.7 h, respectively. The ratio of the metabolite to unchanged risperidone level gradually increased during the experiment with the AUC ratio being significantly greater than unity (2.78). The absolute oral bioavailability in the male Sprague–Dawley rat was 19% for unchanged risperidone while the oral to IV $AUC_{0-\infty}$ (ratio for the active moieties (risperidone+9-OH risperidone) was 52%.

4. Discussion

The aim of this study was to elucidate whether self-assembling mmePEG$_{750}$P(CL-co-TMC) polymeric micelles were able to pass the intestinal barrier after oral administration, and then to assess their biological fate (pharmacokinetics and biodistribution).

Table 2
Pharmacokinetic parameters of unchanged risperidone and its metabolite (9-OH-risperidone) after single intravenous and oral administration of 3 mg/kg risperidone in a 10% solution of [^{14}C]-mmePEG$_{750}$P(CL-co-TMC) micelles (1.0 and 0.2 g/kg for oral and intravenous formulation, respectively) in male Sprague–Dawley rat (mean±SD, n=3)

Drug	Oral administration		Intravenous administration	
	Risperidone	9-OH-risperidone	Risperidone	9-OH-risperidone
Cl (l/h/kg)	–	–	2.2	–
Vd_{ss} (l/kg)	–	–	3.6	–
T_{max} (h)	3	3	–	1
C_{max} (ng/ml or g)	50.0	126	–	154
$t_{1/2,\ 3-8\ h}$ (h)	2.0	2.7	1.2	1.7
$AUC_{0-8\ h}$ (ng h/ml or g)	239	598	1391	519
$AUC_{0-\infty}$ (ng h/ml or g)	265	735	1392	546
Fabs (%)	19	–	–	–
9-OH-risp/risperidone	–	2.78	–	0.39
9-OH-risp+risperidone:				
$AUC_{0-\infty}$ (ng-eq h/ml or g)	999		1911	
$AUC0_{0-\infty\ oral}/AUC0_{0-\infty\ IV}$ (%)	52		–	

The in vitro experiment performed on Caco-2 cells indicates that mmePEG$_{750}$P(CL-co-TMC) block copolymer was capable of crossing an enterocyte monolayer in the absorptive direction proportionally to the incubation time. To our knowledge, it is the first direct demonstration of polymeric micelles uptake across an intestinal model system. This evidence was generated by utilization of polymer containing a chemically stable radioactive monomer (ε-caprolactone doubly labelled with [^{14}C]) and not by using a fluorescent or radioactive group which can modify the polymer structure and behaviour [16–19], or by using micelle-incorporated probes which may dissociate during cell uptake or permeation [20–22].

Passage kinetics for all polymer concentrations were linear during the incubation period. However, the amounts of polymer crossing the monolayer were not proportional to the polymer quantity applied. Indeed, the P_{app} decreased with increasing polymer concentration. This may suggest two hypotheses: 1) only unimers can cross the cell monolayer while micelles, serving as unimers storage, could be transported in a minor way by endocytosis; 2) the polymer is transported in the form of micelles via endocytosis and this pathway is already saturated at polymer concentration just above CMC. Determination of the P_{app} for polymer concentrations below the CMC was not feasible due to the limit of detection.

The mechanisms involved in micelle transport across intestinal mucosa are not well defined but several studies suggest that cellular uptake of polymeric micelles may proceed by pinocytosis [16,20,22]. The fact that mmePEG$_{750}$P(CL-co-TMC) transport is concentration-dependent and drug transport temperature-dependent [13] suggests that micelles can travel through the cell by using the endosomal pathway. An effect of mmePEG$_{750}$P(CL-co-TMC) on tight junctions and thus on cell monolayer integrity was excluded by measuring TEER values, which were stable during the course of the experiment. As mmePEG$_{750}$P(CL-co-TMC) is not cytotoxic [13] and does not modify the TEER value during transport experiment, the polymer transport cannot be directly attributed to an alteration of the Caco-2 monolayer. However, in our in vitro study, notwithstanding that risperidone was entrapped inside the micelles, its P_{app} was 20 folds greater than mmePEG$_{750}$P(CL-co-TMC) P_{app} assuming that the drug and the excipient do not cross Caco-2 monolayer as one. Free risperidone, in equilibrium with entrapped risperidone, seems to be the major absorbed fraction.

To confirm in vivo that mmePEG$_{750}$P(CL-co-TMC) polymeric micelles can cross the intestinal barrier and be absorbed, pharmacokinetic and biodistribution studies were performed in rats. The data clearly demonstrate that mmePEG$_{750}$P(CL-co-TMC)-related radioactivity is absorbed after oral delivery. Indeed, the bioavailability expressed in dose normalized $AUC_{0-72\ h}$-ratio for the total radioactivity was estimated at 40%, indicating that micelles may be orally available.

After their uptake into enterocytes, micelles are very likely released directly to the blood circulation and not via the lymph. Venous drainage from the intestine follows the portal vein and arrives in the liver where it can undergo metabolism whereas components transported in the mesenteric lymph via chylomicrons (essentially long chain fatty acids), drain to the thoracic duct and eventually to the subclavian vein without being subjected to the hepatic first pass effect [23].

The mmePEG$_{750}$P(CL-co-TMC) micelles had a long circulation in the blood ($t_{1/2\ 8-72\ h}$: 28 h) and were not extensively taken up by the reticuloendothelial system (RES). Stealth features are provided to the micelles by the PEG constituents in the shell. PEG chains can diminish opsonization of proteins which activate clearance by the RES by steric hindrance and other mechanism [25–28]. Moreover, as the size of the construct decreases, the uptake by RES decreases [2]. The mmePEG$_{750}$P(CL-co-TMC) micelles did not completely escape this way of blood clearance. Indeed, the extent of uptake of the polymer-related radioactivity is 7.3% and 0.08% of the total administered dose of mmePEG$_{750}$P(CL-co-TMC) in the liver and spleen, respectively, after intravenous administration. This uptake is very low compared with PEG–PCL nanoparticles (size around 200 nm) where approximately 85% of the injected dose in mice is found in the liver within the first hour [24]. This high clearance is common for many kinds of nanoparticles [25–28]. This may be due to the fact that polymeric nanoparticles are much larger than polymeric micelles (size of mmePEG$_{750}$P(CL-co-TMC) micelle: ±20 nm), and therefore, are more susceptible to be cleared from blood by RES macrophages [2].

Excretion of mmePEG$_{750}$P(CL-co-TMC) proceeded by renal elimination because more than 80% of the total administered polymer-related radioactivity was found in the urine after 8 h for the intravenous administration and, around 40% for the oral administration within 24 h matching the percentage of intestinal absorption which was also around 40%.

With a unimeric molecular weight of ±5 kDa and an aggregation number of ±44 (data not shown), the mmePEG$_{750}$P(CL-co-TMC) micelle size is close to the renal filtration limit (20–30 kDa) [3]. This feature can explain the fact that the polymer was still found in the plasma after 72 h, but at a low concentration near to its CMC, assuming the polymer is not extensively metabolised. This may suggest that final disposition requires micelle disassembly into its unimeric components. This finding was also recently reported by Batrakova et al. with the Pluronic® P85 after intravenous administration to mice [29].

Former experiments indicate that the polymer remains stable for several months in water and is slowly degraded in vitro by enzymes (data not shown). However the stability of the polymer in vivo was not studied.

Orally administered risperidone solubilized in mmePEG$_{750}$P(CL-co-TMC) was absorbed. The data would suggest that, to some extent, the micelle is acting as a carrier and that after administration, some degree of dissociation occurs. On the other hand, the polymer could provide a sustained plasma profile for risperidone. In comparison with the oral formulation without mmePEG$_{750}$P(CL-co-TMC) [13], risperidone had a T_{max} delayed 6-fold, and a slightly extended $t_{1/2}$ (1.3-times) when it was coadministered with the polymer. It should be noted that the delayed T_{max} (3 h) for risperidone was similar to

that of the polymer T_{max}. Last but not least, (risperidone + 9-hydroxy-risperidone) bioavailability doubled and reached 52% by the use of 10% mmePEG$_{750}$P(CL-co-TMC) instead of 0.05 M tartaric acid (data not shown).

In conclusion, we demonstrate that self-assembling polymeric micelles containing poorly soluble drug cross the intestinal barrier after oral administration, provide a sustained release of the drug and are eliminated by renal excretion.

Acknowledgements

The Fonds pour la Formation à la Recherche dans l'Industrie et dans l'Agriculture (F.R.I.A.) is gratefully acknowledged for the financial support of Frédéric Mathot. The authors also wish to thank Steve Van Hoegaerden and Willy Verluyten for the HPLC method of the [^{14}C]-labelled mmePEG$_{750}$P(CL-co-TMC) and Cor Janssen for its purity analysis. Additionally, the authors are grateful to CBAT (Somerville, NJ, US) for the polymer synthesis and IWT (Flemish government, Belgium) for the financial support of the initial research program.

References

[1] R. Strickley, Solubilizing excipients in oral and injectable formulations, Pharmaceutical Research 21 (2004) 201–230.
[2] A. Lavasanifar, J. Samuel, G. Kwon, Poly(ethylene oxide)-block-poly(L-amino acid) micelles for drug delivery, Advanced Drug Delivery Reviews 54 (2002) 169–190.
[3] V. Torchilin, Structure and design of polymeric surfactant-based drug delivery systems, Journal of Controlled Release 73 (2001) 137–172.
[4] M.-C. Jones, J.-C. Leroux, Polymeric micelles — a new generation of colloidal drug carriers, European Journal of Pharmaceutics and Biopharmaceutics 48 (1999) 101–111.
[5] K. Kataoka, A. Harada, Y. Nagasaki, Block copolymer micelles for drug delivery: design, characterization and biological significance, Advanced Drug Delivery Reviews 47 (2001) 113–131.
[6] G. Kwon, T. Okano, Soluble self-assembled block copolymers for drug delivery, Pharmaceutical Research 5 (1999) 597–600.
[7] L. Ould-Ouali, A. Ariën, J. Rosenblatt, A. Nathan, P. Twaddle, T. Matalenas, M. Borgia, S. Arnold, D. Leroy, M. Dinguizli, L. Rouxhet, M. Brewster, V. Préat, Biodegradable self-assembling PEG-copolymer as vehicle for poorly water-soluble drugs, Pharmaceutical Research 21 (2004) 1581–1590.
[8] P. Artursson, K. Palm, K. Luthman, Caco-2 monolayers in experimental and theoretical predictions of drug transport, Advanced Drug Delivery Reviews 46 (2001) 27–43.
[9] M. Lindenberg, S. Kopp, J. Dressman, Classification of orally administered drugs on the World Health Organization model list of essential medicines according to the biopharmaceutics classification system, European Journal of Pharmaceutics and Biopharmaceutics 58 (2004) 265–278.
[10] R. Löbenberg, G. Amidon, Modern bioavailability, bioequivalence and biopharmaceutics classification system. New scientific approaches to international regulatory standards, European Journal of Pharmaceutics and Biopharmaceutics 50 (2000) 3–12.
[11] R. Bezwada, S. Arnold, S. Shalaby, B. Williams, Liquid absorbable copolymers for parenteral applications, U.S. Patent 5, 653 992 (A) (1997).
[12] M. Mizutani, S. Arnold, S. Shalaby, Liquid phenylazide-end-capped copolymers of caprolactone and trimethylene carbonate: preparation, photocuring characteristics and surface layering, Biomacromolecules 3 (2002) 668–675.
[13] L. Ould-Ouali, M. Noppe, X. Langlois, B. Willems, P. Te Riele, P. Timmerman, M. Brewster, A. Ariën, V. Préat, Self-assembling PEG-p(CL-co-TMC) copolymers for oral delivery of poorly water-soluble drugs: a case study with risperidone, Journal of Controlled Release 102 (2005) 657–668.
[14] P. Artursson, J. Karlsson, Correlation between oral drug absorption in humans and apparent drug permeability coefficients in human intestinal epithelial (Caco-2) cells, Biochemical and Biophysical Research Communications 175 (1991) 880–885.
[15] B. Remmerie, L. Sips, R. de Vries, J. de Jong, A. Schothuis, E. Hooijschuur, N. van de Merbel, Validated method for the determination of risperidone and 9-hydroxyrisperidone in human plasma by liquid chromatography-tandem mass spectrometry, Journal of Chromatography. B, Biomedical Sciences and Applications 783 (2003) 461–472.
[16] L. Luo, J. Tam, D. Maysinger, A. Eisenberg, Cellular internalization of poly(ethylene oxide)-b-poly(e-caprolactone) diblock copolymer micelles, Bioconjugate Chemistry (13) (2002) 1259–1265.
[17] M. Tobio, A. Sanchez, A. Vila, I. Soriano, C. Evora, J.L. Vila-Jato, M.J. Alonso, The role of PEG on the stability in digestive fluids and in vivo fate of PEG-PLA nanoparticles following oral administration, Colloids and Surfaces, B, Biointerfaces 18 (2000) 315–323.
[18] K. Novakova, M. Laznicek, F. Rypacek, L. Machova, Pharmacokinetics and distribution of ^{125}I-PLA-b-PEO block copolymers in rats, Pharmaceutical Development and Technology 8 (2) (2003) 153–161.
[19] Md. Muniruzzaman, A. Marin, Y. Luo, G. Prestwich, W. Pitt, G. Husseini, N. Rapoport, Intracellular uptake of Pluronic copolymer: effects of the aggregation state, Colloids and Surfaces. B, Biointerfaces 25 (2002) 233–241.
[20] C. Allen, Y. Yisong, A. Eisenberg, D. Maysinger, Cellular internalization of PCL$_{20}$-b-PEO$_{44}$ block copolymer micelles, Biochimica et Biophysica Acta 1421 (1999) 32–38.
[21] D. Maysinger, O. Berezovska, R. Savic, P. Soo, A. Eisenberg, Block copolymers modify the internalization of micelle-incorporated probes into neural cells, Biochimica et Biophysica Acta 1539 (2001) 205–217.
[22] Y.S. Nam, H.S. Kang, J.Y. Park, T.G. Park, S.H. Han, I.S. Chang, New micelle-like polymer aggregates made from PEI-PLGA diblock copolymers: micellar characteristics and cellular uptake, Biomaterials 24 (2003) 2053–2059.
[23] M. Van Greevenbroek, T. de Bruin, Chylomicron synthesis by intestinal cells in vitro and in vivo, Atherosclerosis 141 (1) (1998) 9–16.
[24] D. Shenoy, M. Amiji, Poly(ethylene oxide)-modified poly(e-caprolactone) nanoparticles for targeted delivery of tamoxifen in breast cancer, International Journal of Pharmaceutics 293 (2005) 261–270.
[25] Z. Panagi, A. Beletsi, G. Evangelatos, E. Livaniou, D. Ithakissios, K. Avgoustakis, Effect of dose on the biodistribution and pharmacokinetics of PLGA and PLGA-mPEG nanoparticles, International Journal of Pharmaceutics 221 (2001) 143–152.
[26] D. Bazile, C. Ropert, P. Huve, T. Verrecchia, M. Marlard, A. Frydman, M. Veillard, G. Spenlehauer, Body distribution of fully biodegradable [^{14}C]-poly(lactic acid) nanoparticles coated with albumin after parenteral administration to rats, Biomaterials 13 (1992) 1093–1102.
[27] V. Mosqueira, P. Legrand, J.-L. Morgat, M. Vert, E. Mysiakine, R. Gref, J.-P. Devissaguet, G. Barrat, Biodistribution of long-circulating PEG-grafted nanoparticles in mice: effects of PEG chain length and density, Pharmaceutical Research 18 (2001) 1411–1420.
[28] J.-P. Plard, D. Bazile, Comparison of the safety profiles of PLA$_{50}$ and Me.PEG-PLA$_{50}$ nanoparticles after single dose intravenous administration to rat, Colloids and Surfaces. B, Biointerfaces 16 (1999) 173–183.
[29] E. Batrakova, S. Li, Y. Li, V. Alakhov, W. Elmquist, A. Kabanov, Distribution kinetics of micelle-forming block copolymer Pluronic P85, Journal of Controlled Release 100 (2004) 389–397.